Dalton Transactions

Accepted Manuscript

This article can be cited before page numbers have been issued, to do this please use: Y. Shu and W. Liu, *Dalton Trans.*, 2015, DOI: 10.1039/C4DT03959A.

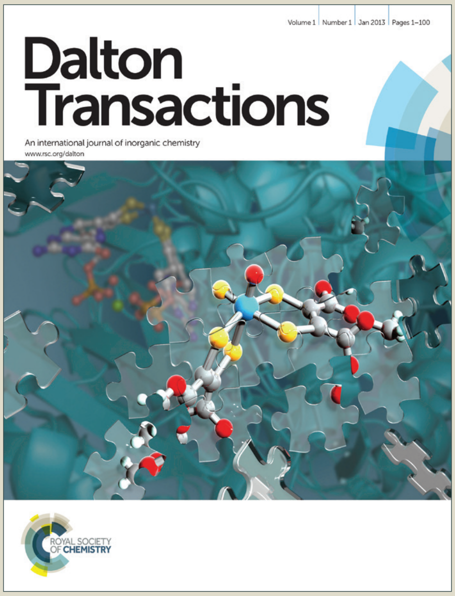

View Article Online
DOI: 10.1039/C4DT03959A

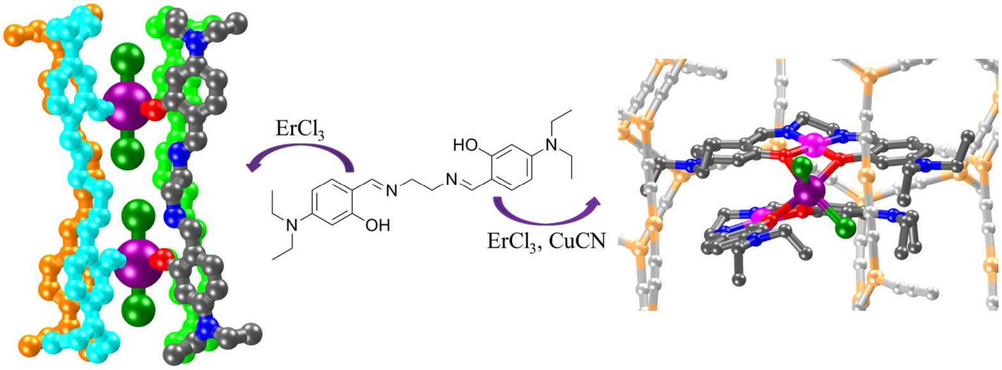

Succeeded in building lanthanide salen “square prism” and in wrapping labile exo-lanthanide salen “double decker” by cuprous cyanide netting. Both lanthanide edifices show near-infrared (NIR) luminescence.
371x138mm (150 x 150 DPI)

View Article Online
DOI: 10.1039/C4DT03959A

Journal Name RSCPublishing

COMMUNICATION

Lanthanide Salen “Square Prism” and Wrapped Exo-Lanthanide Salen “Double Decker”

Cite this: DOI: 10.1039/x0xx00000x

Yu-Bo Shu[a] and Wei-Sheng Liu*[a]

Received 00th January 2012,
Accepted 00th January 2012

DOI: 10.1039/x0xx00000x

www.rsc.org/

An erbium(III) salen “square prism” and a supramolecular aggregate of exo-erbium(III) salen “double-decker” cation wrapped by anionic cuprous cyanide network were prepared from *N,N’*-ethylene bis[4-(diethylamino)salicylideneimine. Both erbium(III) edifices show fine-structure near-infrared (NIR) luminescence under the excitation at visible light area. Here provides a novel and efficient method for stabilizing non-isolable lanthanide edifice in the solid state.

Lanthanide-containing mono- and polymetallic complexes have received extensive attention because of their beautiful architectures and highly desirable properties in optics and magnetism.[1] Recently, great interest has been focused on polynuclear Nd, Er, and Yb(III) lanthanide complexes with near-infrared (NIR) emission around 0.9 to 1.6 μm, due to their potential applications in many advanced technologies such as telecommunication, laser, as well as bio-analysis and imaging.[2] However, the design and assembly of emissive NIR lanthanide edifices remains a real challenge for synthetic chemists, caused by the fact that: (i) most organic ligands (chromophores) are poor sensitizer for NIR lanthanides especially for Er(III) with the smallest energy gap between its excited and ground-state levels that easily matched by the C–H vibrational oscillator,[3] and (ii) lanthanide coordination spheres display high kinetic lability and weak stereochemical preference.[4]

Schiff base or salen ligands are well known for their versatility in the construction of functional metal complexes.[5] The emerging field of study on salen-based complexes is the exploitation of their photophysical properties.[5c] Che and Yersin have reported phosphorescent platinum(II) salen complexes and the application in high-performance organic light-emitting devices (OLEDs).[6] From a series of salen ligands with varying flexible backbones, Yang and Jones has synthesized many visible- and NIR-emissive 4f and d–4f complexes.[7] By design of a chemically modified salen ligand, *N,N′*-ethylene bis[4-(diethylamino)salicylideneimine] (H_2L, Scheme 1), here we report a quadruple-stranded dinuclear lanthanide molecular “square prism” of Er(III) with octahedral metal centers. Two previous examples of structurally characterized quadruply-stranded dinuclear lanthanide edifices have been reported, one is molecular “helicate” of Dy(III) with square-antiprismatic metal centers,[8] and another one is molecular “lanterns” of light and medium lanthanides with monocapped square-antiprismatic metal centers.[9]

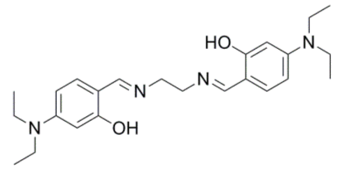

Scheme 1. The H_2L ligand.

An issue often encountered in structural characterization and study on properties is the low stability of lanthanide-containing molecular edifices in the solid state,[4b,10] manifesting as the loss of single crystallinity or even the dissociation of molecule. It is necessary to develop an efficient method for stabilizing and observing valuable edifice molecules. Fujita has succeeded in direct crystallographic observation of extremely labile organic and organometallic species trapped in confined cavities.[11] In our experience, most of polynuclear lanthanide complexes are positively charged. Therefore, we consider wrapping the huge body of lanthanide edifice with cuprous cyanide netting,[12] which is negatively charged due to the necessitation of 3 or 4-connected Cu(I) sites. Then, a supramolecular aggregate of exo-erbium(III) “double-decker” cation caught by anionic cuprous cyanide network is presented.

View Article Online
DOI: 10.1039/C4DT03959A

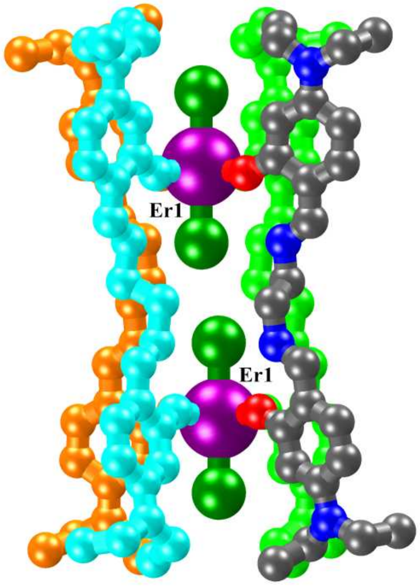

Figure 1. The quadruple-stranded dinuclear "square prism" of complex **1**. Color scheme: Er(III), purple; Cl$^-$, dark green.

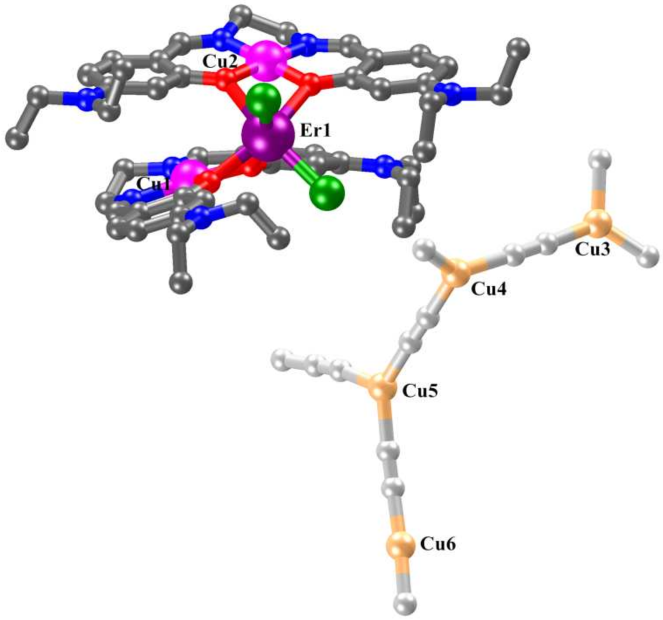

Figure 2. The asymmetric unit of complex **2**. Color scheme: Er(III), purple; Cl$^-$, dark green; Cu(II), pink; Cu(I), pale yellow; C and N of CN$^-$, pale grey.

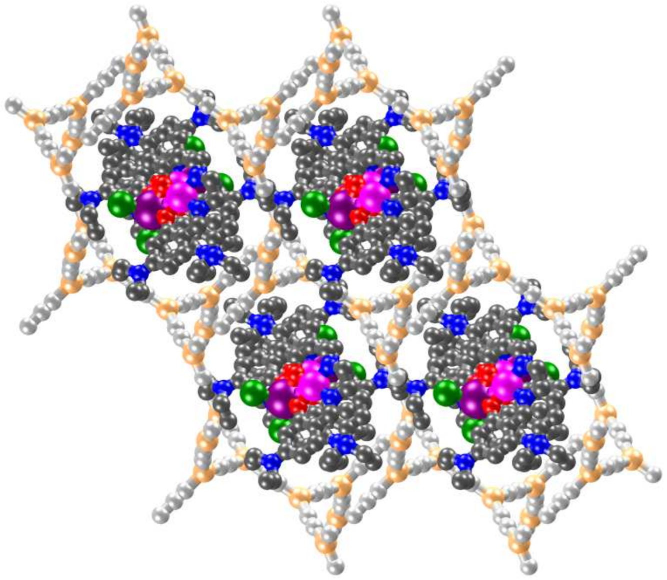

Figure 3. View of the supramolecular aggregate of complex **2** along *b* direction. Color scheme: Er(III), purple; Cl$^-$, dark green; Cu(II), pink; Cu(I), pale yellow; C and N of CN$^-$, pale grey.

Solvothermal reaction of H_2L with $ErCl_3{\cdot}6H_2O$ in methanol solution at 65 °C results in the formation of yellowish-brown polyhedral crystals of $[Er_2(H_2L)_4Cl_4{\cdot}(MeOH)_2Cl_2]$ (**1**). Single-crystal X-ray analysis of **1** at 80 K reveals that it crystallizes in triclinic space group *P-1*. The asymmetric unit contains only one crystallographically independent Er(III) ion. Each Er(III) ion is six-coordinate and adopts O_h octahedron geometry (Figure S4a). In addition to two terminal chlorine anions [Er–Cl1 2.683 Å, Er–Cl2 2.624 Å] at the axial location, the Er(III) ion is equatorially bound to four oxygen atoms [Er–O in the range of 2.200–2.221 Å] from four different H_2L ligands. The four H_2L ligands in turn serve to bridge two adjacent Er(III) ions forming a quadruple-stranded dinuclear molecular "square prism" with the Er···Er separation being *ca.* 8.9 Å (Figure 1). This "square prism" edifice has molecular S_2 symmetry about its center. It should be noted that the ligands (H_2L) remain neutral in the complex through protons migrate from the phenol oxygen atoms to the nitrogen atoms of imine. The valence requirements of the "square prism" molecule are satisfied by the presence of two uncoordinated chloride ions. Each "square prism" interacts with eight neighboring ones through intermolecular π–π stacking and van der Waals force (Figure S5) to generate a 3-D supramolecular framework with the interstices occupied by chlorine counter ions and methanol guest molecules.

Solvothermal reaction of H_2L with $ErCl_3{\cdot}6H_2O$ and Cu^ICN in methanol-acetonitrile solution at 65 °C affords brown-black rectangular block crystals of $[Cu^I_4(CN)_5(CH_3CN)_4{\cdot}ErCu^{II}_2L_2Cl_2]$ (**2**). Single-crystal X-ray analysis of **2** at room temperature reveals that it crystallizes in triclinic space group *P-1*. The asymmetric unit contains four independent Cu(I) ions, two Cu(II) ions, and one Er(III) ion. The Cu(II) ion is generated in situ to fit the square planar N_2O_2 donor set of the L ligand,[13] forming a $Cu^{II}L$ metalloligand with potential *μ*-O donors. The $Cu^{II}L$ unit approachs another one from the side to compose a boat-shape O_2O_2 donor set, which is coordinated to the Er(III) ion [Er–O in the range of 2.277–2.318 Å] (Figure 2). The lastly distorted octahedron coordination geometry of Er(III) is completed by two terminal chlorine anions [Er–Cl1 2.530 Å, Er–Cl2 2.529 Å] (Figure S4b). The formed electropositive $[ErCu^{II}_2L_2Cl_2]$ unit can be described as exo-lanthanide "double-decker" cation, which seems hard to exist alone because of the weak *μ*-O donor. These cations are confined in 1-D rectangular channels that constructed between adjacent 2-D anionic $[Cu^I_4(CN)_5(CH_3CN)_4]_\infty$ networks bearing terminal acetonitrile

View Article Online
DOI: 10.1039/C4DT03939A

ligands (Figure 3). In the 1-D array, the neighboring cations are oriented antiparallel to each other (Figure S6). The cuprous cyanide network exhibits **hcb** (6,3) topology through treating 3-connected Cu(I) ions (trigonal planar coordinated) as nodes and thinking of both CN^- groups and 2-connected Cu(I) ions (linear coordinated) as linkers.

The single crystal of complex **1** is unstable both in mother liquor and in air at room temperature. In-situ powder X-ray diffraction (PXRD) analysis of bulk crystals in air at room temperature shows the fast weathering, but without the change of molecular structure (Figure S2). Thermogravimetric analysis (TG) of weathered sample of **1** under nitrogen atmosphere shows that the "square prism" molecule can be stable up to ~290 °C (Figure S7). Thus, the low stability of complex **1** is merely the easy loss of single crystallinity due to intra- and intermolecular rearrangement in the crystals (e.g., rotation, bending, swinging, sliding, shrinking, or swelling).[14] The single crystal of complex **2** is quite stable at room temperature, and the content of Er(III) ion in bulk crystals can be further confirmed by inductively coupled plasma-atomic emission spectrometry (ICP-AES). TG analysis of complex **2** under nitrogen atmosphere shows that the supramolecular framework is stable up to ~250 °C (Figure S8). As a consequence, we characterized the photophysical properties of both complexes in bulk crystals at room temperature.

The reflectance spectra of complex **1** and **2** are presented in Figure 4. The absorption band of **1** contains two peaks at 305 and 444 nm in regard to $\pi\rightarrow\pi^*$ and intra-ligand charge transfer (ILCT) transitions respectively. The ILCT transition originates from the movement of electron density from the diethylamino group to the imine group in the process of absorption.[6,15] Moreover, weak f→f transitions of Er(III) ($^4I_{15/2}\rightarrow{}^4F_{7/2}$,488 nm; $^4I_{15/2}\rightarrow{}^2H_{11/2}$, 521 nm; $^4I_{15/2}\rightarrow{}^4S_{3/2}$, 546 nm; $^4I_{15/2}\rightarrow{}^4F_{9/2}$, 655 nm; $^4I_{15/2}\rightarrow{}^4I_{9/2}$, 800 nm; $^4I_{15/2}\rightarrow{}^4I_{11/2}$, 978 nm) are observed. The absorption band of **2** consists of $\pi\rightarrow\pi^*$ transition at 323 nm, ILCT transition at 443, and an additional d→d transition of Cu(II) at 678 nm. The excitation spectra of complex **1** and **2** (Figure 5a and 5b) are in good agreement with their reflectance spectra. Complex **1** shows two excitation peaks with one lower than 300 nm and another one at 446 nm. Complex **2** also exhibits two excitation peaks at 350 and 424 nm. The strong visible-light excitation is more desirable as visible light is less likely to damage organic and biological materials.[15,16]

As presented in Figure 5c and 5d, both complex **1** and **2** exhibit fine-structure emission. The $^4I_{13/2}\rightarrow{}^4I_{15/2}$ transition in **1** is split into three components at 1425, 1478, and 1543 nm with a dominant one at the minimum wavenumber (1543 nm), and in **2** the split is at 1425, 1479, and 1549 nm with the maximum at medium wavenumber (1479 nm). These three components reflect the ligand-field splitting of the ground state $^4F_{15/2}$ level under O_h symmetry.[17] The energy barycentre of Er(III) ion shifts toward high wavenumber because of the enhanced Cl–Er (III) ionic bond, and also the increased electrovalence of μ-O–Er(III) bond resulted from the decreased orientation in distorted octahedron coordination environment.[18] Although it is failing to determine the luminescence lifetimes and quantum yields due to the characteristically weak emission of Er(III),[3a] we still identify the stronger luminescence of **1** than that of **2** through comparing their spectral intensities. The weak luminescence of **2** is attributed to the presence of Er(III)→Cu(II) (4f→3d) energy transfer, shown in the hardly observable Er(III) f→f transitions in reflectance spectrum of **2**.[7]

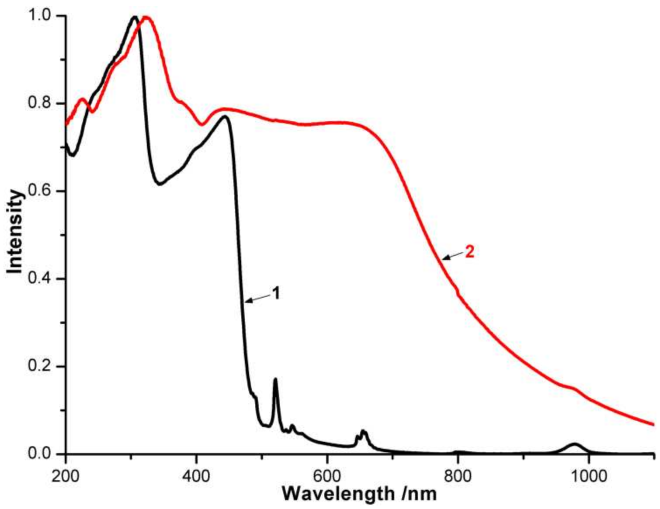

Figure 4. Solid-state reflectance spectra of **1** and **2** at room temperature.

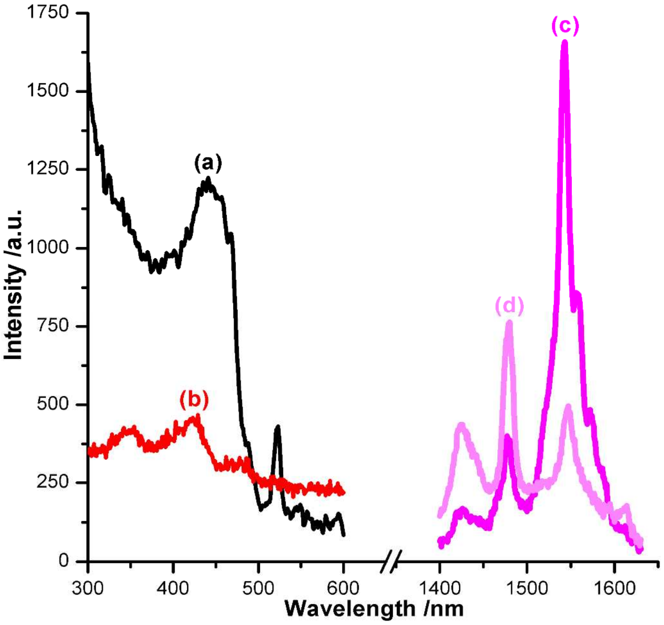

Figure 5. Solid-state excitation and emission spectra of **1** (slit width 9 nm) and **2** (slit width 12 nm) at room temperature. (a) Excitation of **1**, (b) excitation of **2**, (c) emission of **1**, and (d) emission of **2**.

Conclusions

In summary, from a chemically modified salen ligand, we built an erbium(III) molecular "square prism", and thereafter assembled a supramolecular aggregate of exo-erbium(III) "double-decker" cation wrapped by anionic cuprous cyanide network. This is the first attempt of the fabrication of cuprous cyanide network around unstable lanthanide edifice. The fine-

View Article Online
DOI: 10.1039/C4DT03959A

structure NIR emissions of both Er(III) edifices were detected by visible light excitation.

Acknowledgements

The authors acknowledge financial support from the National Natural Science Foundation of China (NSFC) (grant numbers 21431002, and 91122007) and the Specialized Research Fund for the Doctoral Program of Higher Education (grant number 20110211130002).

Notes and references

[a] Key Laboratory of Nonferrous Metals Chemistry and Resources Utilization of Gansu Province and State Key Laboratory of Applied Organic Chemistry, College of Chemistry and Chemical Engineering, Lanzhou University, Lanzhou 730000, P. R. China. E-mail: liuws@lzu.edu.cn

† Electronic Supplementary Information (ESI) available: [IR spectra, PXRD patterns, TG curves, and additional diagrams]. See DOI: 10.1039/c000000x/

Experimental

Synthesis of 1: H_2L (0.010 g, 0.025 mmol) and $ErCl_3 \cdot 6H_2O$ (0.0095 g, 0.025 mmol) were dissolved in MeOH solvent (2 mL). This solution was sealed and heated at 65 °C for 1 day, and then cooled to room temperature. The resulting yellowish-brown crystals were filtered off and dried in air. Yield (based on H_2L): 81%. IR (KBr, cm^{-1}): 3389 (w), 3178 (w), 2970 (w), 2929 (w), 1616 (vs), 1516 (vs), 1387 (m), 1347 (s), 1272 (s), 1241 (s), 1147 (s), 1079 (m), 1014 (m), 968 (w), 848 (m), 779 (m), 703 (m), 587 (m). Elemental analysis (%): calcd for $C_{98}H_{144}Cl_6Er_2N_{16}O_{10}$ (2253.52): C 51.19, H 6.39, and N 9.94; found: C 52.01, H 6.36, and N 9.35.

Synthesis of 2: CuCN (0.0086g, 0.009 mmol) was added to a solution of H_2L (0.010 g, 0.025 mmol) and $ErCl_3 \cdot 6H_2O$ (0.0057 g, 0.015 mmol) in mixed MeOH–MeCN solvent (2/2 mL). After stirring for 5 min, this slurry was sealed and heated at 65 °C for 6 days, and then cooled to room temperature. The resulting brown-black crystals were filtered off and dried in air. Yield (based on H_2L): 75%. IR (KBr, cm^{-1}): 3428 (w), 2968 (w), 2925 (w), 2123 (m), 1596 (vs), 1523 (vs), 1409 (m), 1354 (s), 1327 (m), 1243 (s), 1139 (s), 1075(m), 1015 (w), 974 (w), 829 (m), 792 (m), 705 (m), 644 (m), 587 (w), 563 (w). Elemental analysis (%): calcd for $C_{55}H_{67}Cl_2Cu_6ErN_{14}O_4$ (1607.69): C 41.05, H 4.17, and N 12.19; found: C 40.79, H 4.03, and N 11.82. ICP-AES analysis (%): Er 10.54.

Crystallography analyses: Single-crystal X-ray diffraction data of **1** was collected on an Agilent Technologies Gemini A System (Cu Kα, λ = 1.54178 Å) at 80 K. The data was processed using CrysAlis. Data collection of **2** was performed on a Bruker APEX-II CCD diffractometer (Mo Kα, λ = 0.71073 Å) at 293 K. An empirical absorption correction based on a comparison of redundant and equivalent reflections was applied using SADABS. Both structures were solved by direct methods and refined by full-matrix least-squares cycles on F^2. The Olex2, SHELXS97, and SHELXL97 programs were used for all the calculations.[19] The SQUEEZE program was used to remove the contributions of disordered methanol guest molecules.[20] Crystal data for **1**: $C_{98}H_{144}Cl_6Er_2N_{16}O_{10}$, M = 2253.52, triclinic, space group *P-1*, a = 14.8845(9), b = 15.6342(8), c = 15.6534(11) Å, α = 69.359(5)°, β = 89.180(5)°, γ = 61.857(6)°, V = 2954.4(4) Å^3, Z = 1, Dc = 1.267 g cm^{-3}. The final refinement converges to final R = 0.0792 and wR = 0.2044 with 611 parameters from 11712 independent reflections (I>2σ(I)). The goodness of fit on F^2 was 0.945. Crystal data for **2**: $C_{55}H_{67}Cl_2Cu_6ErN_{14}O_4$, M = 1607.69, triclinic, space group *P-1*, a = 15.091(5), b = 15.687(5), c = 15.948(6) Å, α = 112.308(3)°, β = 98.746(4)°, γ = 108.033(3)°, V = 3161.5(19) Å^3, Z = 2, Dc = 1.689 g cm^{-3}. The final refinement converges to final R = 0.0240 and wR = 0.0589 with 748 parameters from 11115 independent reflections (I>2σ(I)). The goodness of fit on F^2 was 0.973. CCDC reference numbers 1006240 and 1025686.

1 a) J. P. Leonard, P. Jensen, T. McCabe, J. E. O'Brien, R. D. Peacock, P. E. Kruger, T. Gunnlaugsson, *J. Am. Chem. Soc.*, 2007, **129**, 10986; b) K. S. Jeong, Y. S. Kim, Y. J. Kim, E. Lee, J. H. Yoon, W. H. Park, Y. W. Park, S.-J. Jeon, Z. H. Kim, J. Kim, N. Jeong, *Angew. Chem. Int. Ed.*, 2006, **45**, 8134; c) J.-C. G. Bünzli, C. Piguet, *Chem. Soc. Rev.*, 2005, **34**, 1048; d) J.-C. G. Bünzli, C. Piguet, *Chem. Rev.*, 2002, **102**, 1897; e) D. N. Woodruff, R. E. P. Winpenny, R. A. Layfield, *Chem. Rev.*, 2013, **113**, 5110.

2 a) S. V. Eliseeva, J.-C. G. Bünzli, *Chem. Soc. Rev.*, 2010, **39**, 189; b) S. V. Eliseeva, J.-C. G. Bünzli, *New J. Chem.*, 2011, **35**, 1165.

3 a) X.-P Yang, D. Schipper, R. A. Jones, L. A. Lytwak, B. J. Holliday, S.-M. Huang, *J. Am. Chem. Soc.*, 2013, **135**, 8468; b) B.-L. Chen, Y. Yang, F. Zapata, G.-D. Qian, Y.-S. Luo, J.-H. Zhang, E. B. Lobkovsky, *Inorg. Chem.*, 2006, **45**, 8882.

4 a) C. Piguet, J.-C. G. Bünzli, *Chem. Soc. Rev.*, 1999, **28**, 347; b) B. Wang, Z.-P. Zang, H.-H. Wang, W. Dou, X.-L. Tang, W.-S. Liu, Y.-L. Shao, J.-X. Ma, Y.-Z. Li, J. Zhou, *Angew. Chem. Int. Ed.*, 2013, **52**, 3756.

5 a) A. W. Kleij, *Chem. Eur. J.*, 2008, **14**, 10520; b) S. J. Wezenberg, A. W. Kleij, *Angew. Chem. Int. Ed.*, 2008, **47**, 2354; c) C. J. Whiteoak, G. Salassa, A. W. Kleij, *Chem. Soc. Rev.*, 2012, **41**, 622.

6 C.-M. Che, C.-C. Kwok, S.-W. Lai, A. F. Rausch, W. J. Finkenzeller, N. Zhu, H. Yersin, *Chem. Eur. J.*, 2010, **16**, 233.

7 X.-P. Yang, R. A. Jones, S.-M. Huang, *Coord. Chem. Rev.*, 2014, **273**, 63.

8 F. Habib, J. Long, P.-H. Lin, I. Korobkov, L. Ungur, W. Wernsdorfer, L. F. Chibotaru, M. Murugesu, *Chem. Sci.*, 2012, **3**, 2158.

9 Y.-B. Dong, P. Wang, J.-P. Ma, X.-X. Zhao, H.-Y. Wang, B. Tang, R.-Q. Huang, *J. Am. Chem. Soc.*, 2007, **129**, 4872.

10 B. E. Aroussi, S. Zebret, C. Besnard, P. Perrottet, J. Hamacek, *J. Am. Chem. Soc.*, 2011, **133**, 10764.

11 a) T. Kawamichi, T. Haneda, M. Kawano, M. Fujita, *Nature*, 2009, **461**, 633; b) M. Kawano, Y. Kobayashi, T. Ozeki, M. Fujita, *J. Am. Chem. Soc.*, 2006, **128**, 6558; c) S. Horiuchi, T. Murase, M. Fujita, *J. Am. Chem. Soc.*, 2011, **133**, 12445.

12 a) X.-P. Zhou, W.-X. Ni, S.-Z. Zhan, J. Ni, D. Li, Y.-G. Yin, *Inorg. Chem.*, 2007, **46**, 2345; b) J.-Z. Hou, M. Li, Z. Li, S.-Z. Zhan, X.-C. Huang, D. Li, *Angew. Chem. Int. Ed.*, 2008, **47**, 1711.

13 X.-M. Chen, M.-L. Tong, *Acc. Chem. Res.*, 2007, **40**, 162.

14 M. H. Mir, L. L. Koh, G. K. Tan, J. J. Vittal, *Angew. Chem. Int. Ed.*, 2010, **49**, 390.

15 M. H. V. Werts, M. A. Duin, J. W. Hofstraat, J. W. Verhoeven, *Chem. Commun.*, **1999**, 799.

16 Y. Peng, H. Ye, Z. Li, M. Motevalli, I. Hernández, W. P. Gillin, P. B. Wyatt, *J. Phys. Chem. Lett.*, 2014, **5**, 1560.

DOI: 10.1039/C4DT03959A

17 J. C. G. Bünzli, S. V. Eliseeva, Basics of Lanthanide Photophysics, In *Lanthanide Luminescence: Photophysical, Analytical and Biological Aspects* (Eds.: P. Hänninen, H. Härmä), Springer Ser Fluoresc, 2011, **7**, 7.

18 C.-Y. Li, Y.-F. Fan, Change of the coordination field energy levels of Er^{3+} in different chemical environment, *J. Mol. Sci.*, 2001, **17**, 35.

19 a) O. V. Dolomanov, L. J. Bourhis, R. J. Gildea, J. A. K. Howard, H. Puschmann, *J. Appl. Cryst.*, 2009, **42**, 339; b) G. M. Sheldrick, *Acta Cryst. Sec. A*, 2008, **64**, 112.

20 P. Van Der Sluis, A. L. Spek, *Acta Cryst. Sec. A*, 1990, **46**, 194.